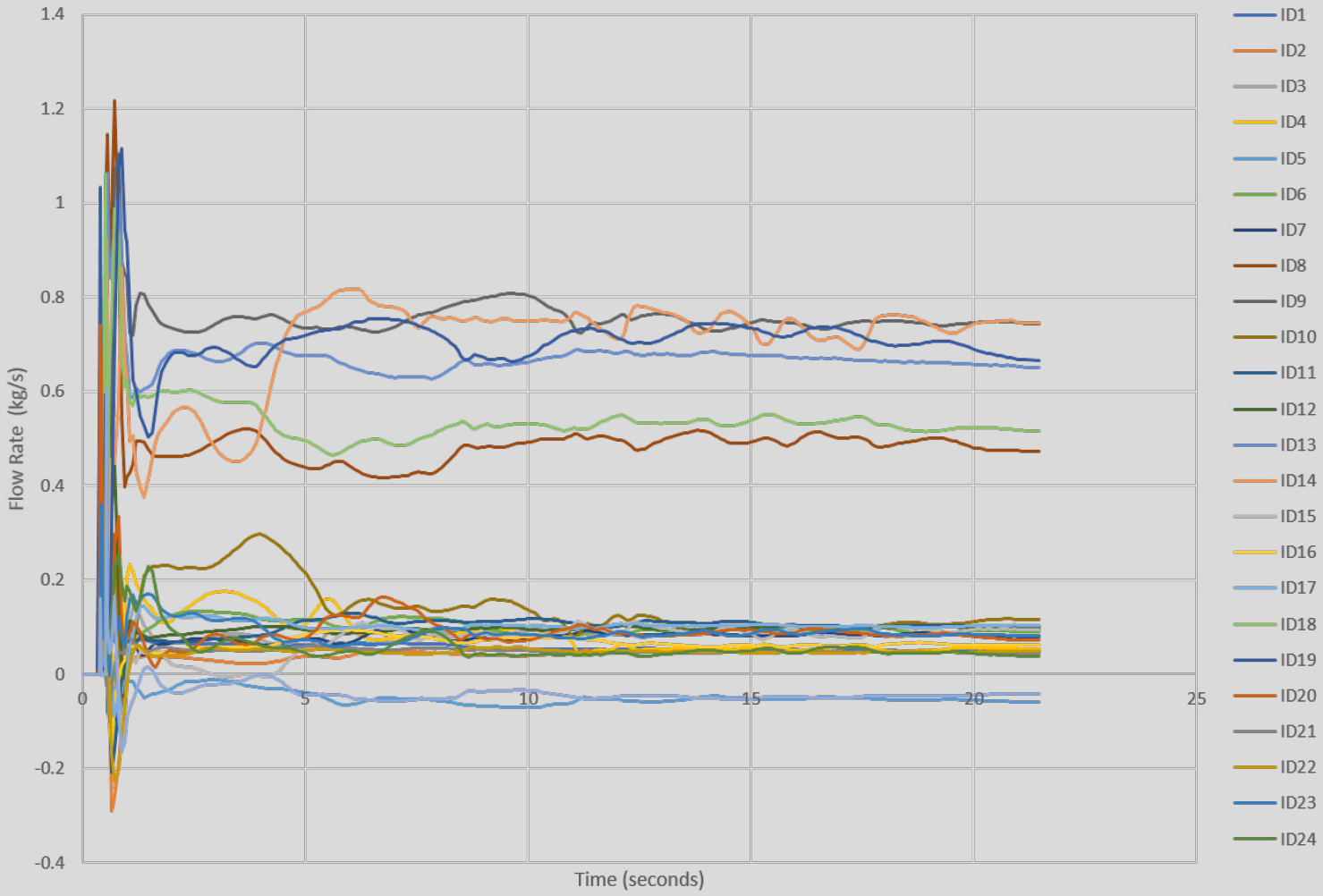

FURTHER EVALUATING IRON FILTER PRINT DESIGNS USING QUANTITATIVE ANALYSES

FOSECO

Author: Tony Midea

Properly filtering iron castings involves utilizing the most optimally engineered filter print and gating system designs to ensure delivery of the cleanest and least turbulent metal to the mold cavity. In 2017, Tony Midea co-wrote a Foundry Practice paper that documented qualitative analyses of filter print designs entitled "Evaluating Iron Filter Print Designs – 30 Years Later"[1]. That paper utilized the most advanced fluid flow technology to assess filter print designs fluid flow characteristics, and to recommend best practice application techniques and methodology to the iron foundry industry.

A follow-on study was undertaken to couple quantitative analyses with qualitative analyses to ensure that the best filter print designs were being recommended. Results from the quantitative analyses shown in this paper support the recommendations from 2017 and provide further insight on best practice filter print designs.

INTRODUCTION

This work focuses on analysis and evaluation of several filter print design concepts[2-10] using casting process simulation software employing sophisticated, first principle fluid flow analysis models. The goal is to investigate problems experienced in foundries and maximize the benefits of filtration to deliver the best possible quality molten metal to the mold cavity, thereby producing high quality castings.

The first section of this paper will provide a summary review of the work documented in the 2017 paper referenced above. This includes the qualitative analyses that involved evaluating fluid flow characteristics within the filtration system to determine best practice.

The second section of this paper will document the methodology used to define the quantitative analyses and provide a detailed examination of the results from the quantitative analyses. The quantitative and qualitative analyses are combined to recommend best practice filter print designs.

METHOD OF ANALYSIS

Standard 75mm x 75mm x 22mm (2.95x2.95x0.866 inch) thick square vertical filter prints were chosen as the baseline for these analyses. Several modifications were made to the filter prints to evaluate the effect of these design modifications on fluid dynamics.

All fluid flow analyses were conducted using MAGMA5 (Version 5.4.0.4) with Solver 5. The mesh size for all simulations was approximately 10 million elements (700,000 metal cells). The metal dataset represents ASTM A536-84 (80-55-06/GGG-60) grade ductile iron poured at 1400°C (2552°F) into a sand mold. The plate casting is approximately 305x610x76mm (12x24x3in) in dimension and approximately 100kg (220lb) in weight. Total pour weight was approximately 110kg (242lb).

The filters were represented using standard 10, 20 and 30ppi, foam filtration pressure drop data for a 22mm (0.866in) thick filter[11]. In all cases, the program was run using the "Automatic Filling Control" feature. Specifically, the program was forced to maintain a pouring cup metal height of 70% for all the simulations, thus ensuring identical pouring conditions for all versions simulated. Fill time was approximately 24 seconds for all configurations, representing a flow rate of approximately 4.5kg/s (10lb/s).
The gating designs evaluated in this report are representative of those in use on industry standard, high pressure, green sand, automated molding equipment.

The choke area was calculated using Equation 1.

$$A = \frac{W}{tDC\sqrt{(2gH}}$$

The top of the sprue was calculated using Equation 2.

$$A_{\text{Sprue Top}} = \frac{V_{PL} \times A_{PL}}{V_{ST}}$$

The sprue was tapered at three degrees to allow for mold stripping.

The runner system follows a ratio of Sprue:Runner:Ingate of 1.0:1.1:1.2
The baseline vertical filter print configuration is shown in Figure 1.

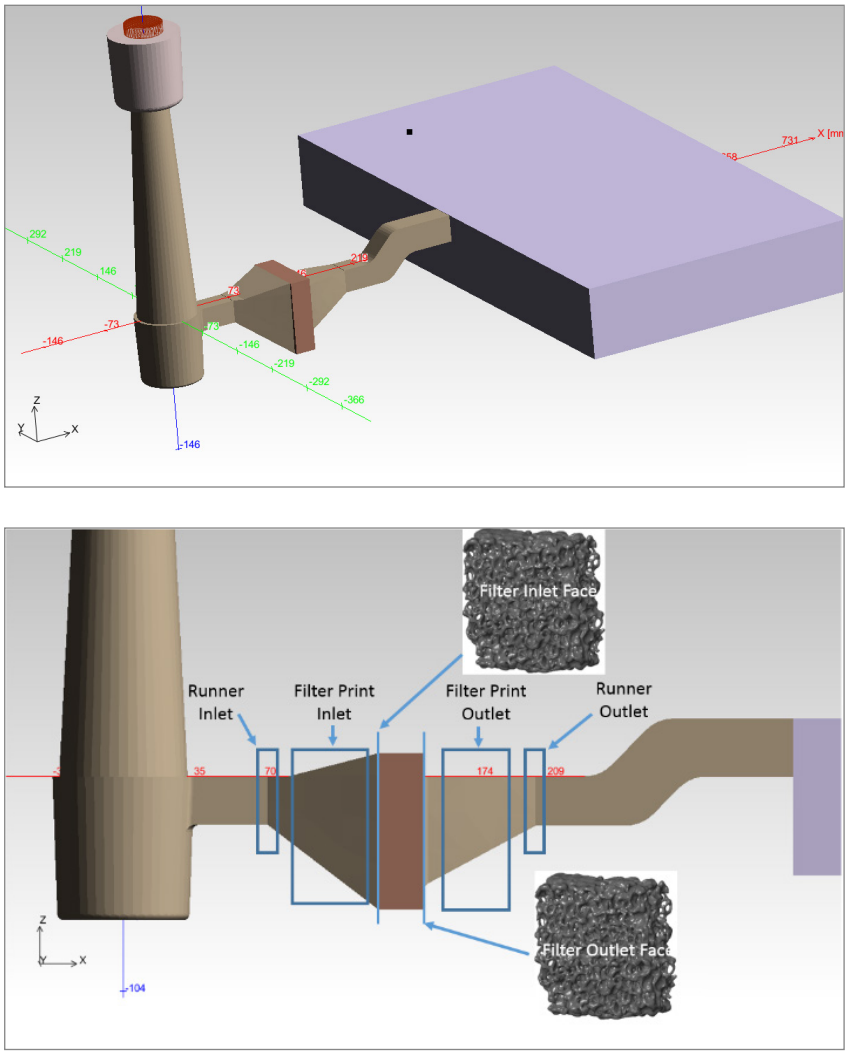

Figure 1. Standard Vertical Filter Print

RESULTS AND DISCUSSION

All fluid flow results shown are analytical and based on the Navier-Stokes flow equations. Flow predictions from this first principal fluid dynamic approach have been validated for several decades in many industries and applications, including molten metal applications. The expectation is that the comparative results shown should be very meaningful and accurate.

QUALITATIVE ANALYSES – SUMMARY REVIEW OF 2017 VERTICAL FILTER PRINT RESULTS

The flow characteristics for a standard vertical filter print are shown in Figure 2. The colors represent flow velocities.

At 10% filled, the flow is steady state in and around the filter print. The color scale ranges from light blue (low velocity, near 0.2m/s (0.66 ft/s)) to white (higher velocity, near 2.0 m/s (6.6 ft/s)). Flow through the filter is approximately 0.3-0.4 m/s (1-1.3 ft/s), and the flow before the filter is laminar, and covers the entire filter. Flow after the filter is uniform and stable.

A cross section through the middle of the filter print at this same time step shows the fluid velocity and flow vectors (Figure 3).

This image clearly shows the uniform flow, and the utilization of the entire filter face for both flow control and filtration. This can be considered a well-designed filter print and gating system that serves as a baseline for this section of the paper.

In application, extreme changes have sometimes been made to standard filter prints to save weight, increase yield and/or fit within pattern plate restrictions. Figure 4 shows one actual example.

While this design results in a 35% weight reduction to the filter print design (0.9kgs, 2lbs), the flow characteristics in the filter print and gating system are adversely affected.

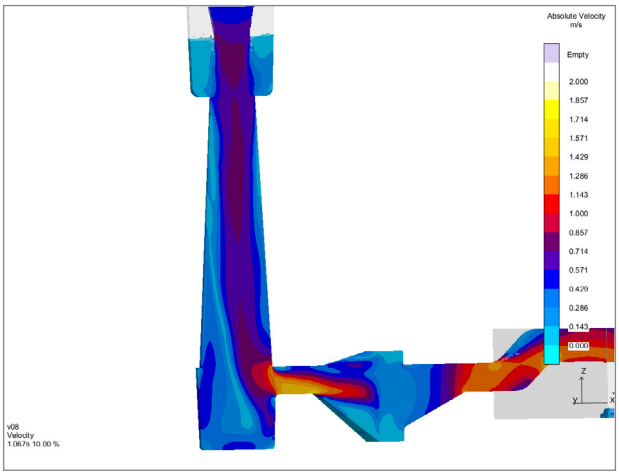

Figure 2. Centerline Cross-Section of Standard Vertical Filter Print Gating System Flow Velocity at 10% Filled

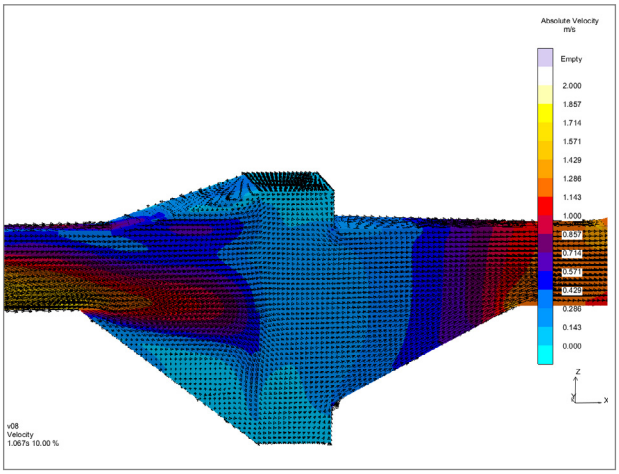

Figure 3. Centerline Cross-Section of Standard Vertical Filter Print Flow Velocity at 10% Filled

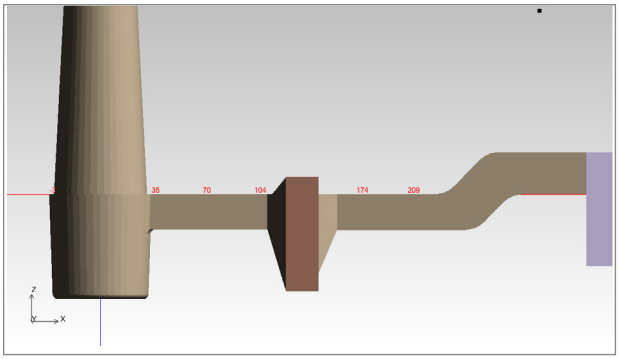

Figure 4. Vertical Filter Print with Filter Print Inlet and Outlet Areas Significantly Reduced

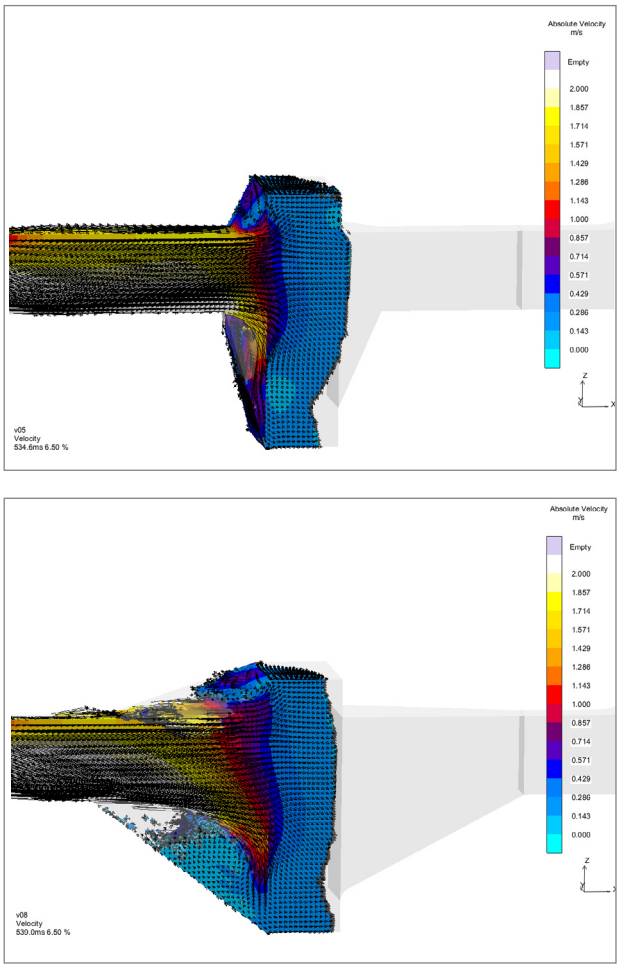

Figure 5. Flow Comparison for Vertical Filter Print with Filter Print Inlet and Outlet Areas Significantly Reduced at 6.5% Filled

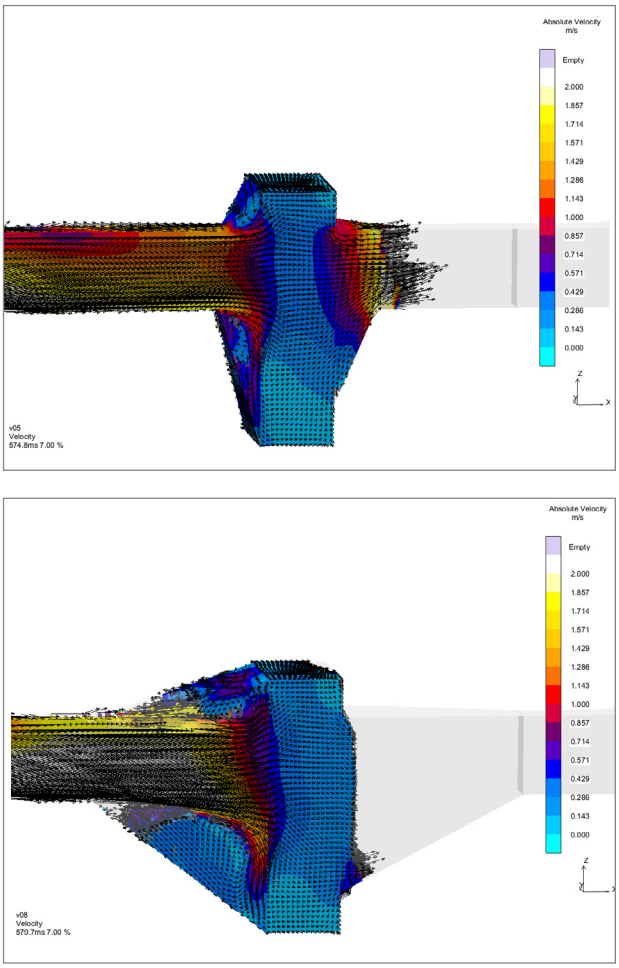

Figure 6. Flow Comparison for Vertical Filter Print with Filter Print Inlet and Outlet Areas Significantly Reduced at 7.0% Filled

Figure 5 shows the flow characteristics at the centerline of the filter print and gating system at 6.5% filled.

(Note: The results for all designs are compared to the standard filter print design results. The standard results are shown as the bottom image in the comparative figures for the vertical filter print examples).

Because of the sharp angles of the modified filter print inlet, the flow accelerates into the center of the filter inlet face and begins to move through the filter before completely filling up the filter print inlet area. The flow characteristics for the standard filter print design show a more evenly distributed flow pattern within the filter print inlet and at the filter inlet face.

The high filter inlet face velocities of the reduced filter print inlet area design results in some very high filter exit face velocities, as shown in Figure 6.

Ideally, the filter should reduce flow energy and turbulence by acting as a flow discontinuity. However, this effect is mitigated if only a small area of the filter is being utilized. This is shown clearly in Figure 6, with the reduced area filter print showing flow exiting the filter at high velocity, while the standard design shows the entire filter filled with metal at very low velocity, and minimal metal flow exiting the filter itself at this time step.

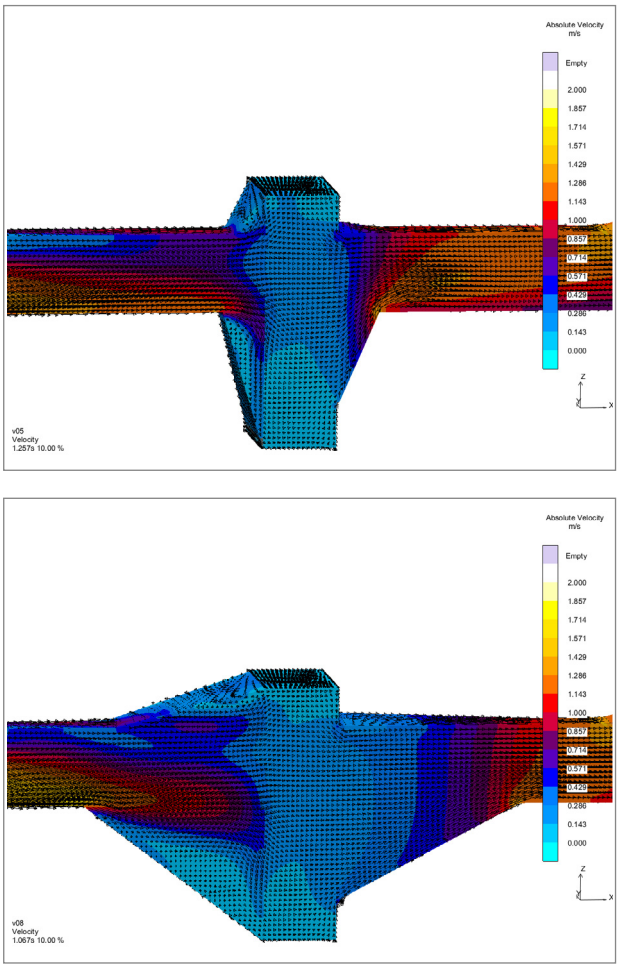

Figure 7. Flow Comparison for Vertical Filter Print with Filter Print Inlet and Outlet Areas Significantly Reduced at 10.0% Filled

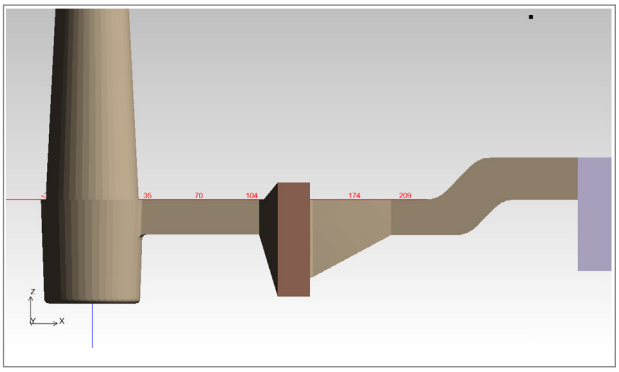

Figure 8. Vertical Filter Print with Filter Print Inlet Area Significantly Reduced

In Figure 7, this continues to be the case even at steady state flow.

Even at steady state, the reduced area filter print design is not allowing the entire filter print inlet area to be used, and instead is pushing the metal through the center of the filter. This results in non-uniform flow behind the filter, and the potential for turbulence. Contrast this with the uniform flow profile shown for the standard filter print design, particularly at the filter outlet face, the filter print outlet and downstream in the runner.

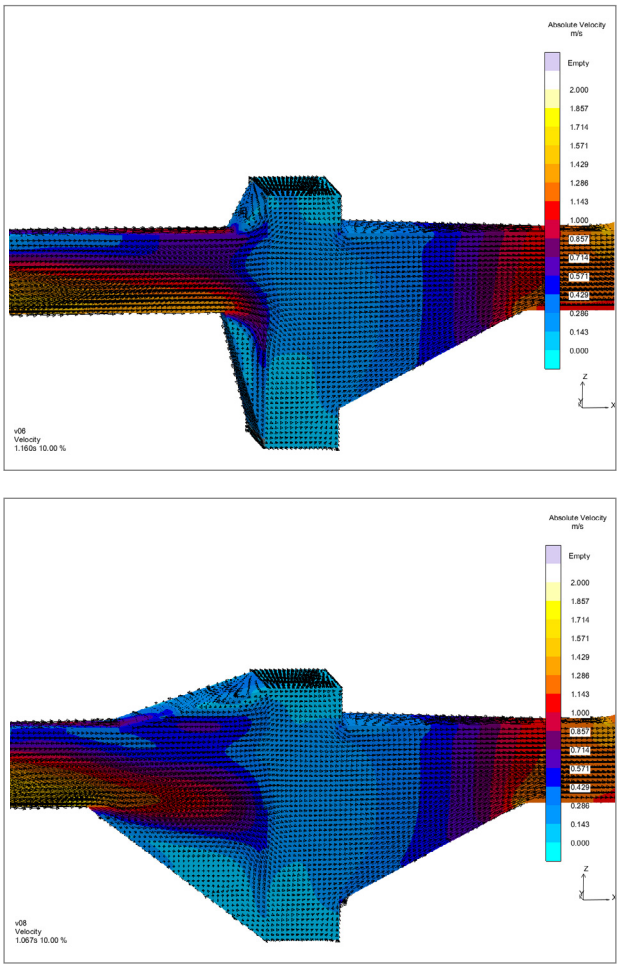

Figure 9. Flow Comparison for Vertical Filter Print with Filter Print Inlet Area Significantly Reduced at 10.0% Filled

Reducing the area of the filter print in this fashion to slightly increase yield (0.9kg, 2lbs saved) has significant adverse effects on the flow characteristics in the filter print inlet, the filter inlet face, the filter outlet face, the filter print outlet, and in the downstream runner bar. This type of alteration is not recommended for best practice filter print design.

Figure 8 shows a configuration with the area of the filter print outlet modified to match the standard print shown in Figure 1, but the reduced filter print inlet area is unchanged.

In this case, the issues in the filter print inlet area and at the filter inlet face remain the same as discussed previously, but the flow after the filter shows clear improvement. In Figure 9, note how similar the filter outlet face and filter print outlet flow profiles appear when comparing the reduced filter print inlet area configuration with the standard filter print.

The main difference between this configuration and the standard filter print is the dramatically higher flow velocities at the filter inlet face for the reduced area design, and the fact that only a small portion of the filter is being used. This is the same situation discussed in the previous configuration, but the yield argument is even more clear this time.

Reducing the area of the filter print inlet only saves 0.6kg (1.3lb), but adversely affects the flow such that the entire filter area is not being used to efficiently filter inclusions from the metal. Again, this small yield improvement has a significant adverse effect on the flow and is not recommended in practice.

Figure 10 shows a similar design with the area reduced at the filter print outlet only.

Reducing the area of the filter print outlet only will save just 0.3kg (0.66lb), and results in very poor flow exiting the filter print. The flow comparison is shown in Figure 11.

In this case, the flow in the filter print inlet and at the filter inlet face has the same beneficial characteristics as that of the standard filter print. However, the flow at the filter outlet face, within the filter print outlet and in the downstream runner bar exhibits the same poor characteristics shown in Figures 5-7. A filter print design that adversely affects the flow characteristics and delivers minimal yield improvement should not be considered as practical.

Figure 12 shows the standard configuration with an addition of a slag trap before the filter.

This change only adds approximately 0.23kgs (0.5lbs) to the filter print design, but results in a positive impact on the overall flow characteristics of the filter print itself.

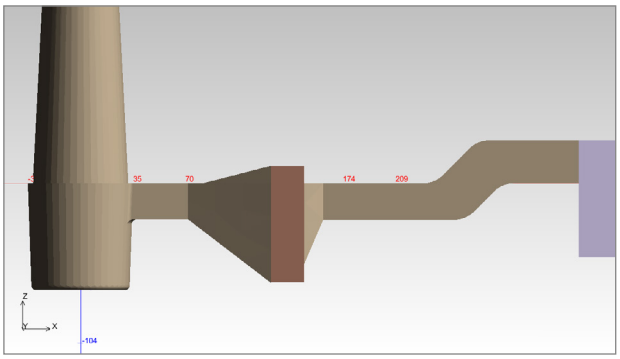

Figure 10. Vertical Filter Print with Filter Print Outlet Area Significantly Reduced

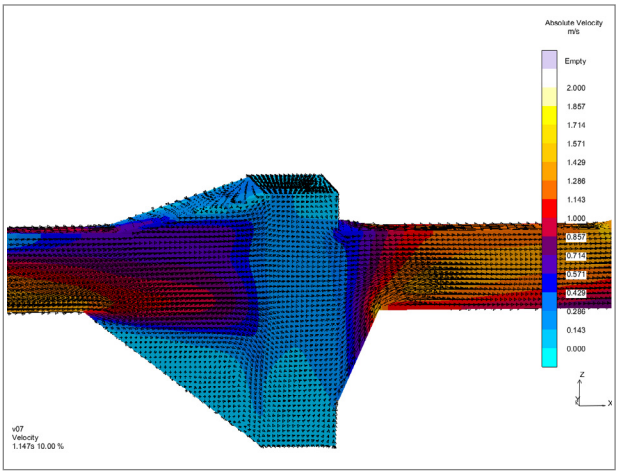

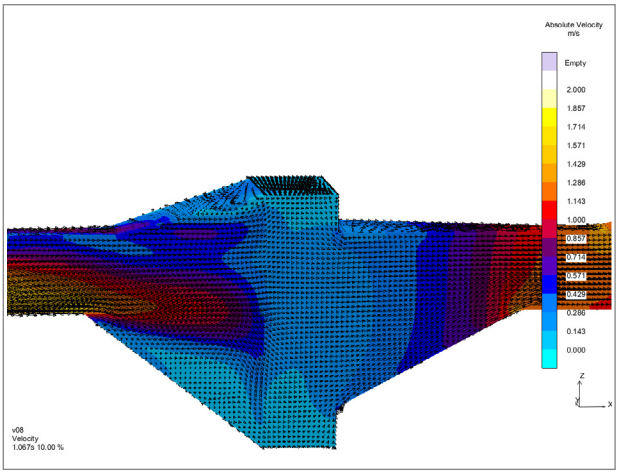

Figure 11. Flow Comparison for Vertical Filter Print with Filter Print Outlet Area Significantly Reduced at 10.0% Filled

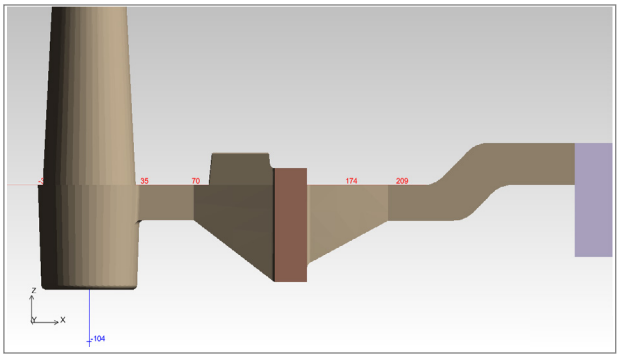

Figure 12. Standard Vertical Filter Print with Slag Trap

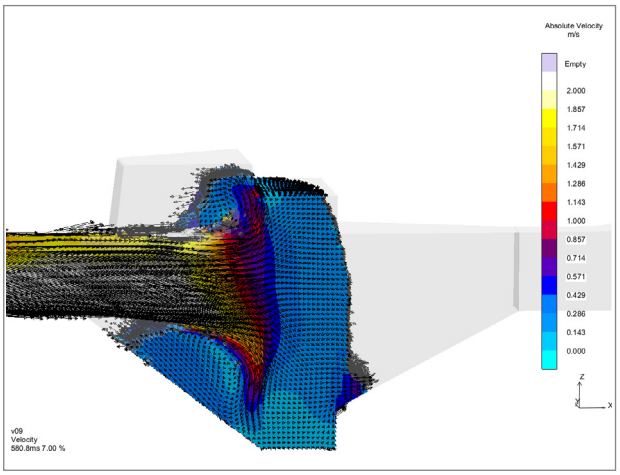

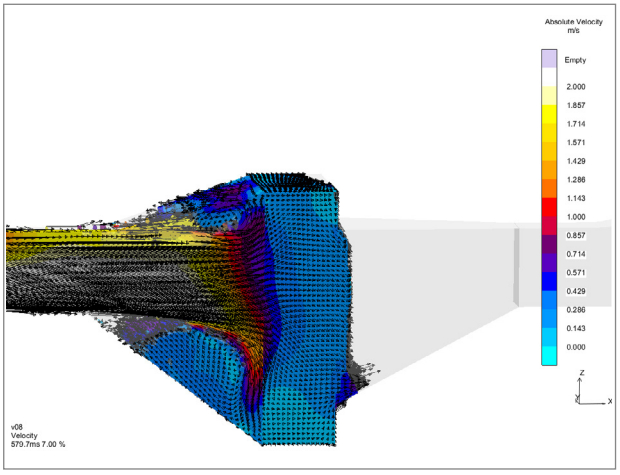

Figure 13. Flow Comparison for Standard Vertical Filter Print with and without Slag Trap at 7.0% Filled

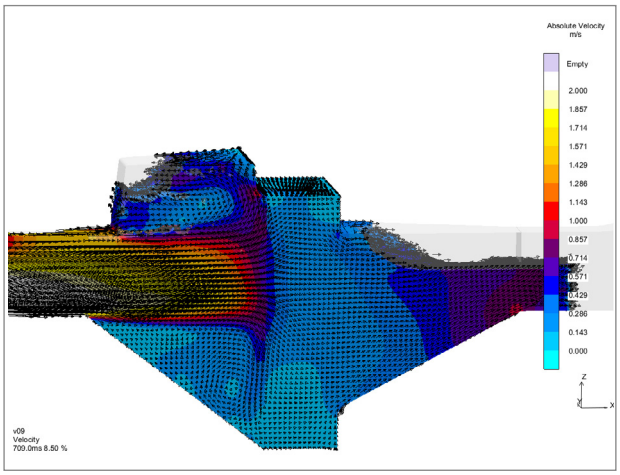

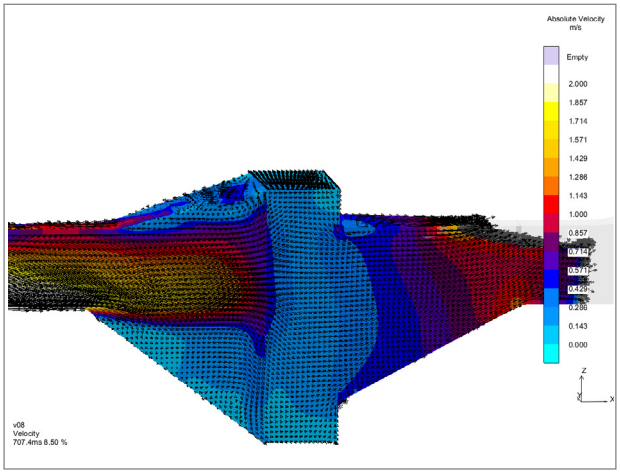

Figure 14. Flow Comparison for Standard Vertical Filter Print with and without Slag Trap at 8.5% Filled

The filter print with a properly designed slag trap displays the same the high-quality flow characteristics shown in the standard filter print with the added benefit of better filter print inlet flow and potentially better filtration efficiency. Figure 13 shows how the trap begins to work as soon as the metal reaches the filter.

Note that the bottom of the filter print inlet has filled quickly, and that the flow is washing the filter inlet face and moving upwards into the slag trap area.

At 8.5% (Figure 14), the flow is nearly stabilized, and the slag trap is forcing the initial metal into a beneficial counter-clockwise eddy current, thus potentially allowing inclusions to reverse direction and slowly float upward into the trap. The standard filter print without the slag trap also has a small area of beneficial eddy currents at the top of the filter print inlet, but very little space to trap and retain inclusions.

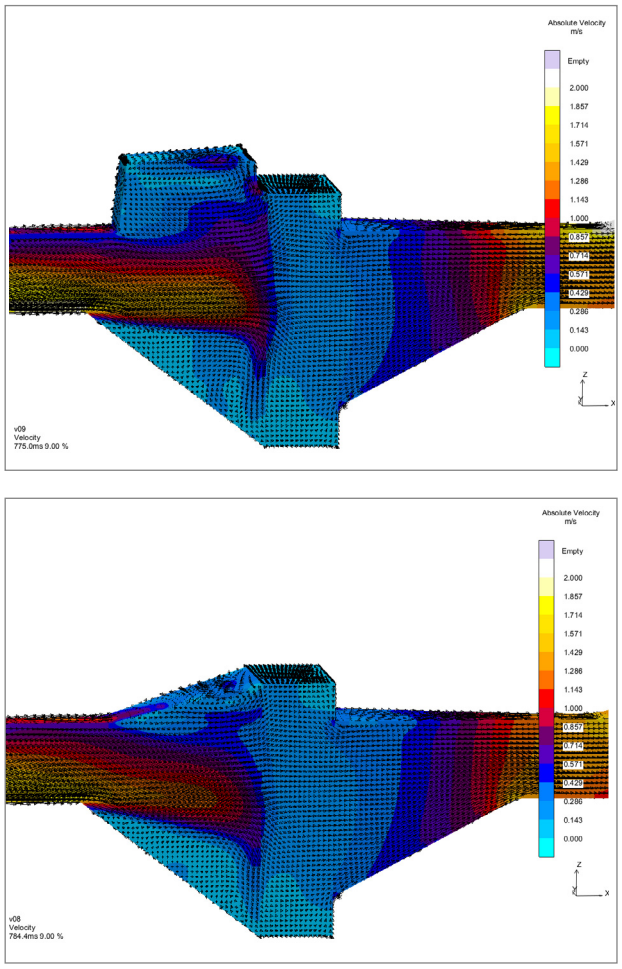

Figure 15. Flow Comparison for Standard Vertical Filter Print with and without Slag Trap at 10.0% Filled

By 10% filled (Figure 15), the filter print is fully stabilized and any inclusions that entered the slag trap will remain.

Adding a small area to trap slag in the filter print inlet improves the flow characteristics of the runner design and the ability of the filter print to trap inclusions. These are significant benefits for a minimal reduction in yield.

To summarize, the conclusions from the 2017 qualitative analyses were that the standard filter print design with a slag trap was the preferred design, followed by the standard filter print without a slag trap, if adding a trap was prohibited by pattern plate real estate issues. Sharp angles within the filter print itself were not recommended.

QUANTITATIVE ANALYSES – FILTER PRINT FLOW NUMERICAL RESULTS

Qualitative, comparative analyses, like the ones shown thus far in the paper, can provide powerful, convincing imagery of gating system changes that positively or negatively affect metal flow characteristics. Historically, comparative analyses between gating systems have provided sufficient evidence to trial and implement concepts and designs that improve metal flow and casting quality. However, an engineer is inclined to evaluate design concepts analytically, and assign absolute values with visuals. In effect, an engineer desires to combine a quantitative analysis with a qualitative analysis. That is the gist of the remainder of this paper which presents new, novel approaches and results.

Previously, only 10ppi SEDEX* filters were evaluated for the five filter print designs. For the quantitative analysis, 10, 20 and 30ppi filters will be evaluated for these five designs such that the DOE now consists of 15 separate configurations.

A good quality filter print should utilize as much of the filter area as possible and distribute the flow velocity as evenly across the filter face as possible. This allows the filter to control the flow and maximize capacity.

A novel approach to evaluate filter face flow rate was taken using the ingate options within the software. Normally, ingate material is assigned to the geometry component that connects the runner bar to the casting. In turn, the software allows for metal flow rate to be recorded for all materials identified as ingate material for the entire filling cycle.

Figure 16 shows how 25 separate ingates were modeled, just in front of the filter, such that flow rate could be evaluated for 25 discrete sections of the filter face itself.

Each numbered ingate produces a corresponding flow rate curve and allows for quantitative assessment of the variation of flow across the entrance side of the filter face.

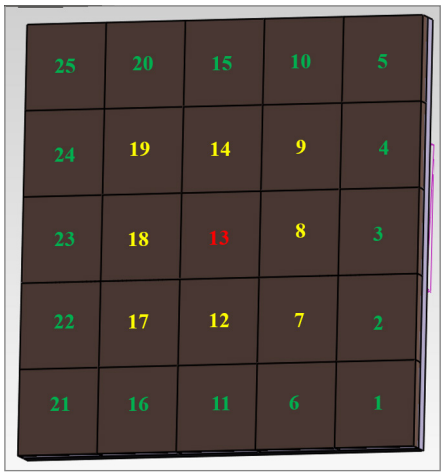

Figure 16. Ingate Array Attached to Filter Face (image courtesy of Matt Jacobs and Konstantin Nikolov, MAGMA Foundry Technologies, Inc.)

Figure 17 shows the flow rates (kg/s) for all 25 ingate locations on the filter face for the standard filter print design with a 10ppi filter.

Most of the flow is entering the filter at six central ingate locations, namely 8, 9,13, 14, 18 and 19.

A review of this same filter print design with 20 and 30ppi filters shows a similar pattern, with an exception. There is a slight reduction in flow velocity at ingates 13 and 14 with increasing porosity for all filter print designs.

Figure 18 shows the flow rates (kg/s) for all 25 ingate locations on the filter face for the filter print design with reduced entrance/exit areas and with a 10ppi filter.

The flow rate at location 14 is much higher (0.94 kg/s or 2.1 lb/s) than for the standard filter print design (0.75 kg/s or 1.65 lb/s). During filling, approximately 25% more metal flows through location 14 for this filter print design as compared to the standard filter print design (23 kg vs 18 kg, or 50 lb vs 40 lb). Most of the flow for this filter print is moving through locations 9, 13, 14 and 19, which constitutes usage of a relatively small section of the filter face.

A review of this same filter print design with 20 and 30ppi filters shows a similar pattern with similar exceptions listed previously.

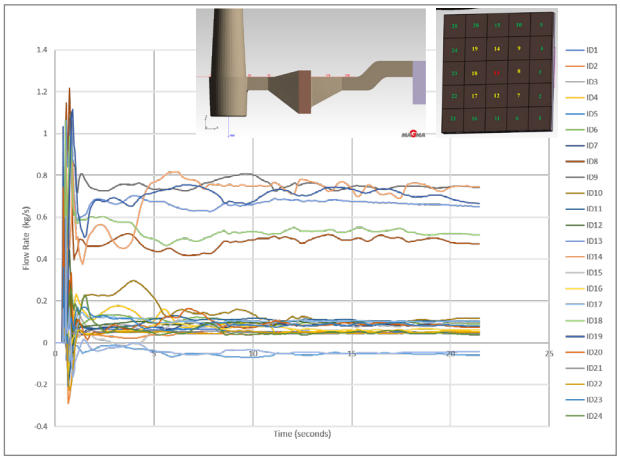

Figure 17. Standard Filter Print Flow Rates Across Inlet Face

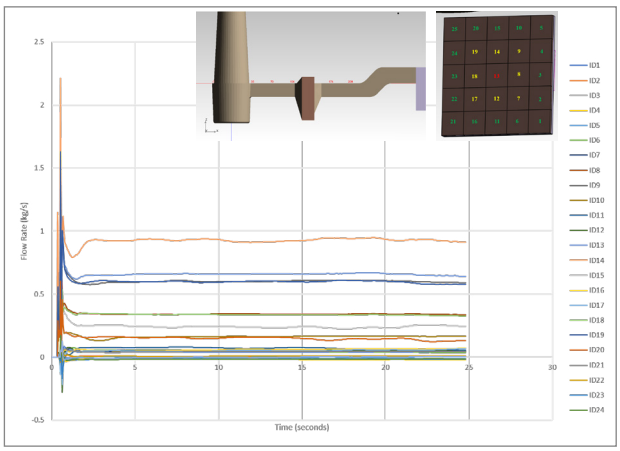

Figure 18. Reduced Area Filter Print Flow Rates Across Inlet Face

Another novel idea was implemented to quantitatively assess the angularity of the flow within the filter print. In Figure 19, two "reference" flow vectors were established, one before the filter, one after.

The flow reference direction criterion allows for the setting of a reference direction to compare to calculated flow results, and most importantly, to determine angle deviation from flow in the x-direction.

During filling, the flow vector deviance from 0 degrees along the x-axis is calculated for each mesh element at each time step during the entire filling process. Average and maximum deviation angle are calculated and used for quantitative comparison of the different designs.

Figure 20 gives a graphic example of the angle deviation calculation.

High angle deviation is directly related to higher turbulence in the filter print. An angle deviation of 90 degrees is flow that is perpendicular to the reference flow. A value of 180 degrees is backflow, or fluid flow completely opposite the flow reference direction. Low angle deviation can be considered laminar, quiescent flow.

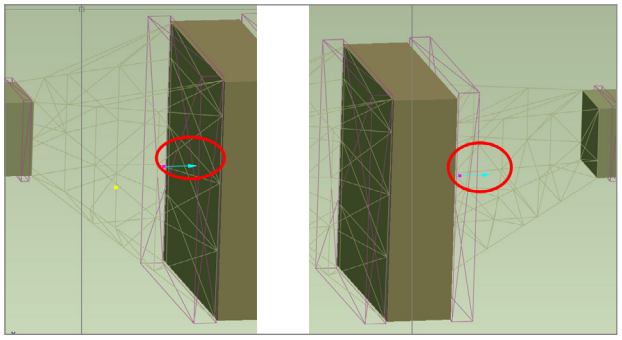

Figure 19. Flow Reference Direction Criterion
(image courtesy Matt Jacobs, MAGMA Foundry Technologies, Inc.)

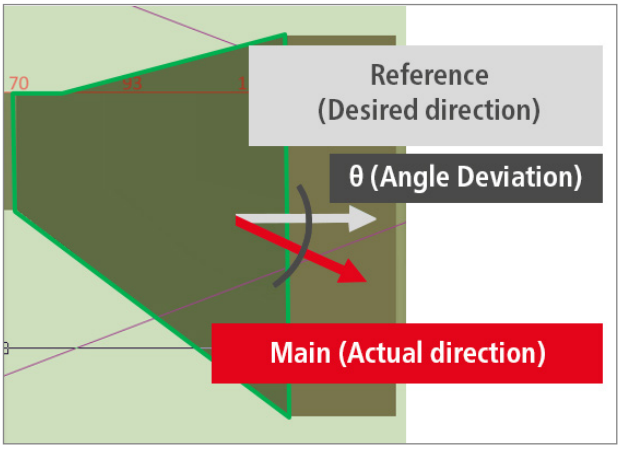

Figure 20. Flow Reference Direction Calculation
(courtesy Konstantin Nikolov, MAGMA Foundry Technologies, Inc.)

The most powerful part of the evaluation is conducted using the "parallel coordinates" tool, which allows the engineer to review the effects of a filter print design on the multiple criteria at the same time. Figure 21 shows the comparison prior to analysis.

The designs are shown on the far right. Each calculated criterion is given a unique y-axis, and the values are shown with the criterion labeled at the top of the graph. The colored lines are used to connect the criterion scores for each design, and each design has a uniquely colored line. Lower scores are desired over higher scores for each criterion in this analysis.

From left to right, the objectives are:

- Average angle deviation after the filter
- Average angle deviation before the filter
- Maximum angle deviation after the filter
- Smooth filling (described later)

(Note: The maximum angle of deviation before the filter objective results are not useful because they include the effect of eddy currents at the top of the filter print and into the slag trap. Therefore, these results are not included in this analysis.)

In all cases, the desire is to minimize the values of these objectives.

The first action is to pull down the "Design" red arrow to show results for only filter print designs 1 through 5, which represents the 10ppi filter results (Figure 22).

Angle deviation after the filter is more important than angle deviation before the filter because: a) the filter will ultimately force the flow towards the x-axis and b) some flow angularity is desired before the filter to help wash inclusions off the face of the filter to float and stick on the sand at the top of the runner bar, or into the slap trap, if one exists.

After the filter, it is imperative to minimize the angularity to reduce the possibility for turbulent flow.

(In general, angularity before and after the filter, while necessary to go from the small cross-section runner bar to the filter print or from the filter print exit to the runner bar, should be minimized.)

The largest discrepancies seen in this analysis occur after the filter with respect to the maximum angle deviation. Designs 3 and 5 (with the reduced filter print exit area) have maximum angle deviation values of approximately 174-176 degrees, meaning that some part of the flow after the filter is moving upstream, or in the negative x-direction. This is obviously not ideal, as was shown qualitatively and discussed in detail in the 2017 paper.

These two designs are eliminated (Figure 23) by moving the "MAX Dev POSTFILTER" red arrow down below 174 degrees.

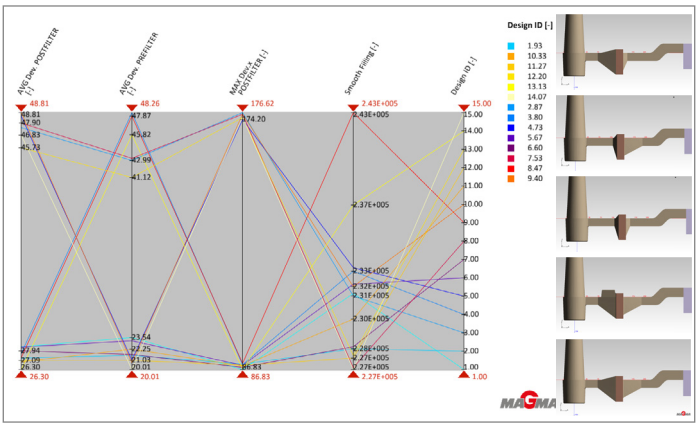

Figure 21. Parallel Coordinates Quantitative Results

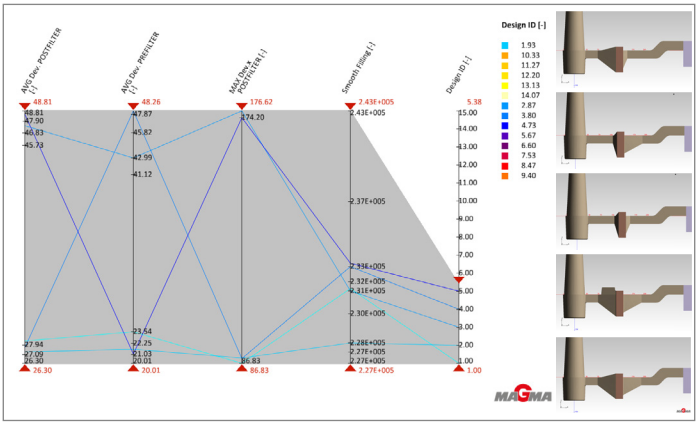

Figure 22. Parallel Coordinates Quantitative Results for 10ppi Filters

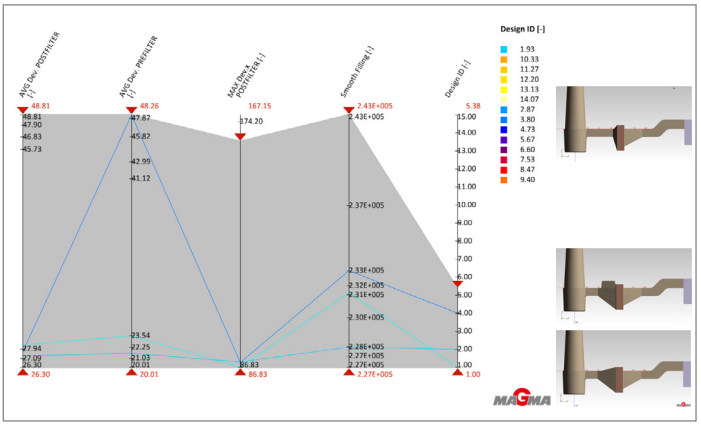

Figure 23. Parallel Coordinates Quantitative Results for 10ppi Filters – Elimination Round 1

All the other filter print designs have a maximum angle deviation after the filter of no more than 86 degrees.

The "smooth filling" criterion is defined as the maximum free surface of the cast alloy. It is a measure of metal front interaction with air, and thus the potential for inclusions.

By moving the "smooth filling" red arrow down below 2.33e05 (Figure 24), Design 4 is eliminated.

Surveying the two remaining designs, Design 2 (with the slag trap) has slightly better (lower) objective values than Design 1.

Further lowering the "smooth filling" objective red arrow below 2.31e05 eliminates Design 1 leaving Design 2 as the clear winner of the quantitative analysis (Figure 25).

The conclusion that Designs 1 and 2 are superior, with Design 2 being the best is consistent between the qualitative and quantitative analyses.

Does filter porosity alter these conclusions? No. This identical design elimination procedure, as shown in Figures 23-25 would yield the same conclusions for the 20ppi filter configurations (Designs 6-10) and the 30ppi filter configurations (Designs 11-15). As a result, this part of the analysis is not explicitly shown here but can be inferred from the next analysis.

One final analysis shows the effect of different ppi filters on the objectives calculated absolute values (Figure 26).

Each design has three of the same color curves representing the 10, 20 and 30ppi filter results.
Moving the "MAX Dev POSTFILTER" red arrow down to 171 degrees shows all the results for filter print Designs 1, 2 and 4 (Figure 27).

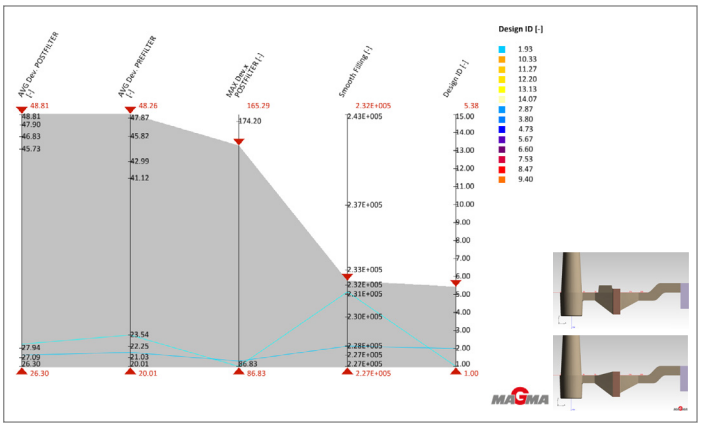

Figure 24. Parallel Coordinates Quantitative Results for 10ppi Filters – Elimination Round 2

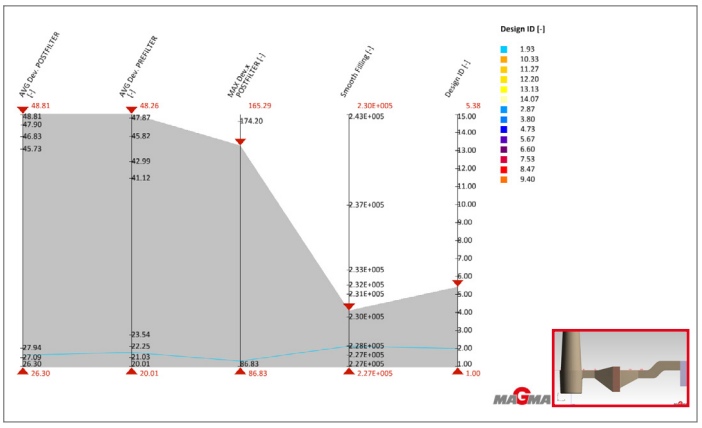

Figure 25. Parallel Coordinates Quantitative Results for 10ppi Filters – Elimination Round 3

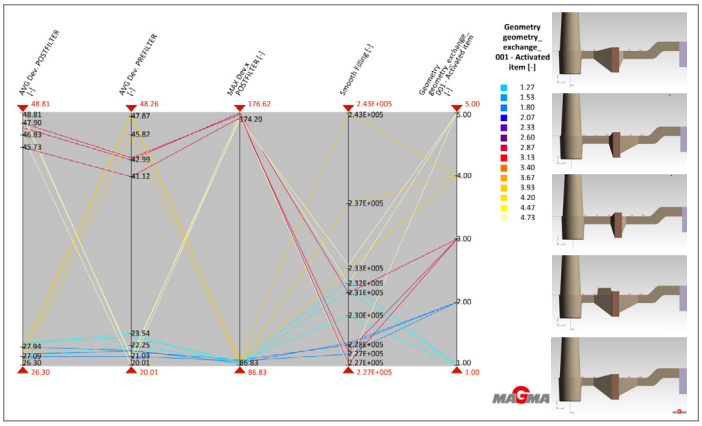

Figure 26. Parallel Coordinates Quantitative Results for All Filters

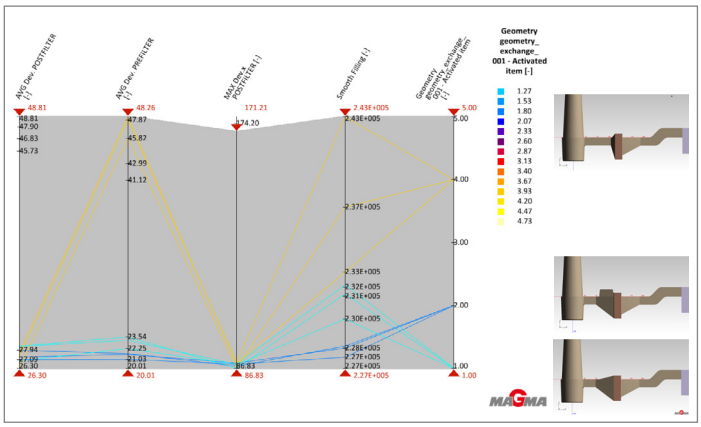

Figure 27. Parallel Coordinates Quantitative Results for All Filters – Designs 1, 2 and 4

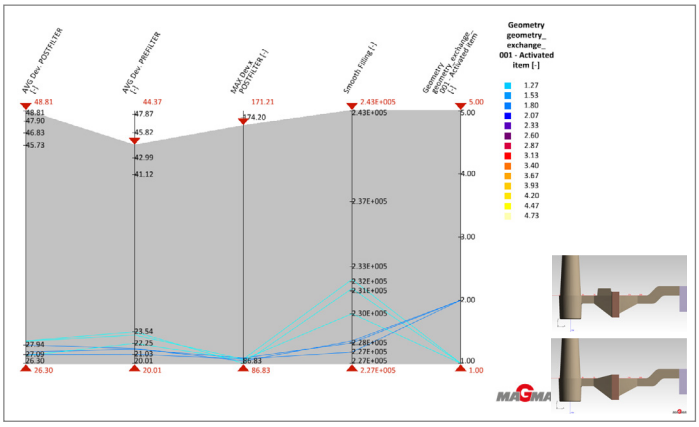

Figure 28. Parallel Coordinates Quantitative Results for All Filters – Designs 1 and 2

Moving the "AVG Dev PREFILTER" red arrow down to 44 degrees (Figure 28) shows all the results for the two best filter print designs (1 and 2).

Figures 26, 27 and 28 reveal several important points.

First, the results shown earlier are confirmed, namely that filter porosity does not alter the conclusions that Designs 1 and 2 are optimal for this analysis.

Second, there is some variability in the calculated objective results related to filter type for non-optimal designs such as Designs 3, 4 and 5, thus implying that there is some variability in performance for these designs dependent upon foam filter restrictiveness.

Third, Figure 28 shows that the foam filter restrictiveness has very little influence on the calculation of quantitative objectives for this study for the best filter print designs (1 and 2). Therefore, the best filter print designs from this analysis are independent of the restrictiveness of the foam filtration device employed.

CONCLUSIONS

Alterations are sometimes made to standard filter prints to improve yield without careful analysis of the effect on the fluid flow properties on the gating system. Quantitative analyses and the previously documented qualitative analyses evaluated the effect of several filter print design changes on the quality of metal flow in the filter print, the runner system and through the filter itself.

In general, the conclusions are as follows:

- Quantitative and qualitative analyses align to conclude
  - o Filter print Design 2 is recommended
    - Includes slag trap
  - o Filter print Design 1 is second best if pattern real estate prohibits the inclusion of a slag trap
  - o Both designs maximize the use of the front face of the filter with respect to flow rate
  - o Both designs maximize filter capacity
  - o Both designs reduce flow angularity (turbulence) before and after the filter, thus maximizing flow uniformity

- Best practice filter print design is independent of reticulated foam filter restrictiveness
  - o Caveat: filter geometry was represented using a pressure drop boundary condition

- Large reductions in filter print inlet and outlet areas, and sharp angles within the print itself adversely alter the flow characteristics resulting in non-uniform flow and turbulence
  - o Yield improvement is minimal
  - o Not recommended

Future work is planned to review additional design concepts and to validate these configurations with molten metal.

ACKNOWLEDGMENTS

The author wishes to thank Matt Jacobs and Konstantin Nikolov at MAGMA Foundry Technologies, Inc. for their ideas, their assistance with creating models and objectives, conducting lengthy simulations and their contributions to the analyses.

This paper was originally published by AFS.
AFS Paper Number 20-053, published April 2020.

REFERENCES

1. Dickinson, B., Adams, A., Midea, T., "Evaluating Iron Filter Prints – 30 Years Later", AFS Transactions, 17-027, (2017).
2. Giebing, S., Baier,, A. "SEDEX – Process Reliability Through Effective Quality Control," Foundry Practice, vol. 254, pp. 4 (June 2011).
3. Morales, R.D., Adams, A., Dickinson, B. "Enhancing Filtration Knowledge to Improve Foundry Performance", Foundry Practice, Special Edition, pp. 21 (May 2008).
4. Baier, A. "The Influence of Filter Type and Gating System Design on the Machinability of Vertically Parted Grey Iron Castings", Foundry Practice, Special Edition, pp. 29 (May 2008).
5. Taylor, K.C., Baier, A. "Application of SEDEX Ceramic Foam Filters on Vertically Parted Moulds Such as Disamatics", Foundry Practice, vol. 238, pp. 10 (March 2003).
6. Brown, J.R. "Foseco Ferrous Foundryman's Handbook", pp. 250-266, Butterworth-Heinemann, Woburn, MA, 2000.
7. Park, W.H. "SEDEX Ceramic Foam Filter Applications in Korea", Foundry Practice, vol. 221, pp. 2 (March 1991).
8. Matsuo, H. "SEDEX Ceramic Foam Filter Applications on Regular Production Casting in Japan, Foundry Practice, vol. 220, pp. 4 (September 1990).
9. Kallisch, W. "SEDEX – A Filter with Authority", Foundry Practice, vol. 217, pp. 18 (April 1989).
10. Rietzscher, R. Sipl. – Ing. "The Filtration of Molten Iron", Foundry Practice, vol. 212, pp. 5 (March 1986).
11. Heine, R.W., Loper, C.R., Rosenthal, P.C. "Principles of Metal Castings", pp. 223, McGraw-Hill Book Company, New York, 1967.
12. Midea, A.C. "Pressure Drop Characteristics of Iron Filters", AFS Transactions, 01-042, (2001).

CONTACT

TONY MIDEA
REGIONAL SIMULATION MANAGER - AMERICAS, JAPAN AND SOUTH KOREA

Tony.Midea@vesuvius.com
+1 440 863 2762

All statements, information and data contained herein are published as a guide and although believed to be accurate and reliable (having regard to the manufacturer's practical experience) neither the manufacturer, licensor, seller nor publisher represents or warrants, expressly or impliedly:

(1) their accuracy/reliability
(2) that the use of the product(s) will not infringe third party rights
(3) that no further safety measures are required to meet local legislation

The seller is not authorised to make representations nor contract on behalf of the manufacturer/licensor.
All sales by the manufacturer/seller are based on their respective conditions of sale available on request.

COMMENT
Editorial policy is to highlight the latest Foseco products and technical developments. However, because of their newness, some developments may not be immediately available in your area.

Your local Foseco company or agent will be pleased to advise.

FOSECO

Foseco International Limited
P.O. Box 5516
Tamworth
Staffordshire
England B78 3XQ
Registered in England No. 468147

VESUVIUS